QUARTERLY REPORT NO. 1
CONTRACT JPL 952129

ION ENGINE THRUST VECTOR STUDY

APRIL 1968

HUGHES
HUGHES AIRCRAFT COMPANY

HUGHES RESEARCH LABORATORIES • MALIBU

HUGHES RESEARCH LABORATORIES
Malibu, California

a division of hughes aircraft company

ION ENGINE THRUST VECTOR STUDY

Quarterly Report No. 1
JPL Contract 952129

G. R. Brewer, K. Amboss,
G. Nudd, H. King, R. Seliger, and
S. Kami

April 1968

This work was performed for the Jet Propulsion Laboratory, California Institute of Technology, as sponsored by the National Aeronautics and Space Administration under Contract NAS 7-100.

This report contains information prepared by Hughes Research Laboratories under JPL subcontract. Its content is not necessarily endorsed by the JET Propulsion Laboratory, California Institute of Technology, or the National Aeronautics and Space Administration.

TABLE OF CONTENTS

LIST OF ILLUSTRATIONS

ABSTRACT

The purpose of this investigation is to establish the probability that thrust vector misalignment will occur in an ion thruster array. To accomplish this it is necessary to establish first the probability that any combination of a number of possible mechanical perturbations in the system may occur, second to investigate the effect of such perturbations on the ion trajectories, and finally to interpret this information in terms of thrust variations for a single thruster and the array of thrusters. This report discusses progress made during the first three months of a nominal two year program to conduct the above investigation by a combined analytical-experimental technique.

I. INTRODUCTION AND SUMMARY

As a result of comprehensive studies over the past three years, the design of solar powered electric propulsion systems for interplanetary missions is becoming more crystallized. It is known, for example, that the thruster array will involve a cluster of perhaps eight to twelve thrusters arranged on a frame which can be translated in two directions (or other suitable freedom of motion) relative to the spacecraft. This translational motion is necessary in order to assure that the center of thrust will pass through the center of mass of the spacecraft, for any configuration of active and inactive thrusters. The thrust vector of an individual thruster will not necessarily be along the thruster axis and could change slightly in magnitude and direction with time. The effect of these misaligned thrust vector components around the pitch and yaw axes can be negated by the translation mechanism mentioned above; the component around the roll axis, however, can be compensated only by the spacecraft attitude control system. Therefore, it is of considerable importance to SEP spacecraft design to know the expected thrust vector misalignment as a function of various thruster operational parameters, mechanical displacements, and time. Such knowledge is also fundamental to the development of techniques for reducing the changes in the thrust vector. The objective of this program is the establishment, by analysis and subsequently by experiment, of an expected change in thrust vector from an electron bombardment engine, as a result of all known or anticipated causes. The first phase of this program is devoted to the analysis of expected electrode displacements, determination of the effects of these displacements on the ion trajectories and thereby on the thrust vector, and the design of apparatus for experimental verification, in Phase II.

This report covers the first three months of this contract. For the purposes of conducting the program and reporting, the work is divided into four major tasks: (1) the ion optical study, to be concerned with the determination of ion trajectories as a function of electrode misalignment;

(2) analysis of the causes and magnitudes of the expected electrode misalignment and later the determination of the total thrust vector as the summation of the contributions of the individual holes; (3) the design of the thruster to be used in Phase II for experimental verification, and (4) the design of the instrumentation to be used in the experimental work in Phase II; this last task includes the thrust stand and the electrode position monitor and motion generator.

During this first quarter the electrolytic tank system was used to conduct some initial studies on the effects of electrode placement on the ion optical properties of the accelerator structure. The resulting data were used as the basis for digital computer analysis of the ion trajectories and shape of the ion source. A considerable effort was expended in modifying the available digital computer program to make it applicable to this problem. This program has been checked out and is now running satisfactorily. In analyzing the effects and causes of electrode misalignment, it was decided that more accuracy could be achieved by determining certain of the thermal data needed in the analysis from an experimental test. Thus, a thruster was instrumented with simulated heat sources and thermocouples, and the experimental test was started.

The design parameters of the thruster to be used for experimental verification of the analysis were chosen and the thruster designed. Weight and performance were estimated.

The instrumentation to be used for the experimental verification tests of thrust misalignment in a later program phase, includes the thrust stand and the devices to simulate electrode motion and to measure these displacements. After an analysis of a number of different techniques for measuring thrust misalignment, the thrust stand was chosen as the method best able to satisfy the accuracy requirements. A thrust stand concept, based on the displacement of a thin quartz rod, with error signals generated by the HRL bubble tilt sensor, was analyzed in detail during this quarter. This concept was found to be quite satisfactory;

however, two separate experiments would have to be performed in order to determine all desired components of thrust vector misalignment. Late in the quarter a new thrust stand concept was conceived which is simpler and is capable of measuring simultaneously all desired thrust components. Detailed analysis of this device is being carried out. The electrode position monitor and motion generator are being designed; preliminary tests have been conducted in order to aid in finalizing the choice and detailed design.

II. ION OPTICAL STUDY

A. General Objectives and Approaches

The total thrust from an ion engine consisting of an array of apertures is given by the time rate of change of the momentum of the ion particles exhausted from it. The velocity, and hence momentum, of each ion is determined by the electric fields it experiences during its motion. Thus a perturbation of these fields caused by an electrode misalignment will perturb the total thrust (magnitude and direction) of the engine. The ion optical study is directed toward determining the exhaust momenta of the ions for various electrode perturbations, and thus determining the variation in thrust vector caused by electrode misalignment.

The approach for this study is to calculate the ion trajectories for a single perturbed aperture and to obtain the total thrust vector by summation for all apertures in the engine. A number of basic electrode misalignments that can be considered are illustrated in Fig. 1.

In Fig. 1(a) the electrode spacing is decreased while the rotational symmetry is preserved. This will result in an increase in the magnitude of the thrust from this aperture, which may cause the direction of the thrust vector from the engine as a whole to rotate. In Fig. 1(b) the electrodes are displaced normal to the beam axis, thus destroying its symmetry and causing a change in the magnitude and direction of the thrust vector. The case illustrated in Fig. 1(c) can be considered as the sum of the two effects above, which alters both the magnitude and direction of thrust vector.

It can be seen that the rotational symmetry of the flow generally will be destroyed and the perturbed flow will be noncircular, formed about a curvilinear axis. It is not possible, in general, to determine this type of flow exactly either with the analog or digital computer. It is intended that a full solution be formed by a suitable combination of a axisymmetric solution and a planar solution.

In most problems involving space charge flow the boundary conditions are prescribed on a given surface on which the potential variation or the normal derivative is specified. Problems involving plasma boundaries involve a "free" surface in the sense that the location of the boundary must be found, given the nominal potential variation and the normal derivative. This problem can be solved only by specifying a boundary contour and by refining it in an iterative manner. Experimental conditions can be changed rapidly in the electrolytic tank; for this reason it is convenient to use it to obtain an approximate solution which is subsequently refined on the digital computer.

B. Choice of Ion Optical System

The basic factor in choosing the ion optical system to be analyzed was that it should be representative of the current state of the art in terms of both electrical performance and mechanical structure. This leads directly to the choice of round apertures in a hexagonal close packed array, as described below. Such a system (in a number of forms) has been standard for many years, has been studied both analytically and experimentally, and has successfully passed many thousands of hours of life testing. The exact dimensions were arrived at in conference with the JPL program manager and were based on data available from HRL and JPL programs, as well as the extensive parametric studies and life tests conducted at LeRC in the development program leading to the SERT II thruster.[1] The main criteria were the following.

1. Maximum Open Area in Screen Electrode

SERT II investigations, recently confirmed at HRL, indicate that maximizing the open area in the screen electrode improves thruster performance. A practical upper limit is 70% open area; above this point the apertures must be drilled so close together that the structure becomes very fragile both to fabricate and to launch. Screen electrode apertures of 0.187 in. diameter, spaced 0.210 in. on centers, were chosen.

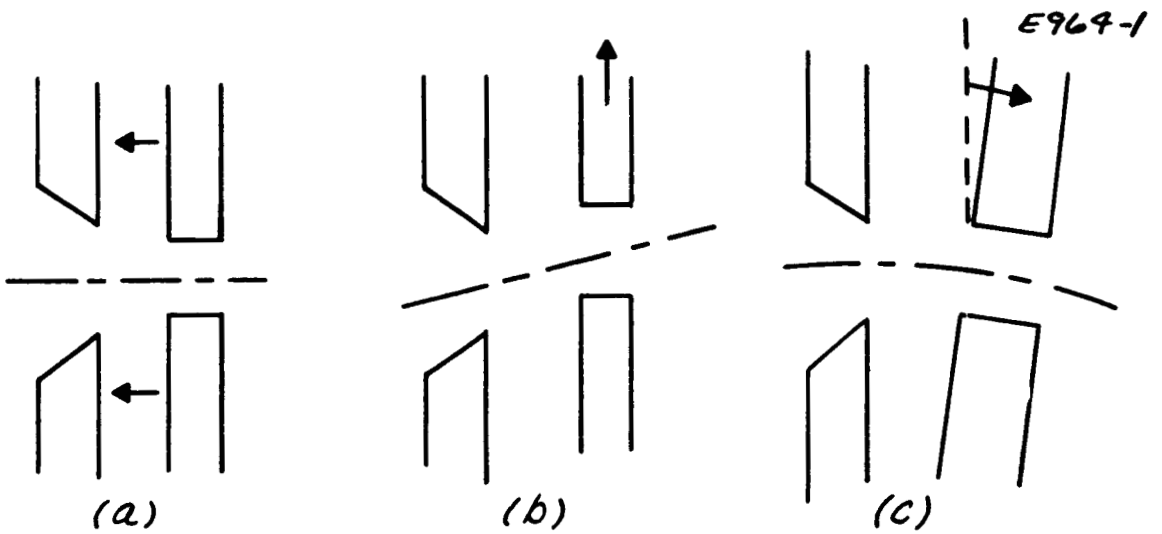

Fig. 1. Basic electrode misalignments.

2. Thin Screen Electrode

Studies at JPL have indicated that reducing the thickness of the screen electrode results in improved performance. A thickness of 0.030 in. was chosen as a practical minimum.

3. Tapered Screen Apertures

It has been shown that countersinking the screen apertures on the plasma side results in an optical element whose perveance varies, depending on the position of the plasma sheath, to accommodate variations in current density as a result of plasma density variations in the discharge chamber. It is planned to countersink the electrodes used here, although the thinness of the screen and thin web between apertures will reduce the benefits of the countersinking.

4. Accelerator Aperture Size

It has been demonstrated that the apertures in the accelerator electrode may be smaller than those in the screen electrode and still provide a high perveance design. This is desirable because the web between apertures is then thicker than in the screen electrode. The additional mass improves heat conduction and increases the electrode lifetime, which is limited ultimately by sputter erosion. Based on an analytical HRL study the accelerator aperture diameter was chosen as three-fourths of the screen electrode diameter (here 0.144 in.).

5. Accelerator Thickness

The accelerator must be massive enough to remain integral under sputtering as a result of charge exchange ion bombardment for 10^4 hours — a typical mission duration. Because the aperture diameter and center-to-center aperture spacing have been defined above, only the thickness can be adjusted to provide the necessary mass. The following assumptions were made:

- Thruster diameter, 30 cm
- Beam current = 1200 mA

- Beam voltage = 1100 V (I_{spe} = 3000 sec)
- Accelerator current = 0.5% = 60 mA
- Sputtering rate 3.5 g/A-hour (Ref. 2) .

Therefore, in 10^4 hours, 210 g of material will be sputtered away.

If it is further assumed that the beam intensity is four times as great at the center as at the edge of the beam and that a safety factor of 2.5 is necessary to reliably prevent electrode failure, the accelerator electrode thickness may be calculated to be 0.110 in. For weight reduction, the thickness of the accelerator electrode may be radially varied to conform approximately to the radial plasma density variations — hence the anticipated radial variation in sputter erosion. Under the above assumed 4 to 1 plasma density variation, the accelerator is then 0.028 in. thick at the circumference, providing a weight saving of slightly more than 1 lb.

6. Screen-Accelerator Spacing

The spacing between the screen and accelerator electrodes is nominally 0.090 in. This value was based on the HRL electrolytic tank study completed prior to this contract, as well as experimental data. It is desirable, however, to increase the perveance of the ion optical array by reducing this distance to the point at which either the quality of the ion optical system becomes unacceptably poor because of the large aspect ratio or the electrodes actually touch or arc over under some operating conditions. With these factors in mind, the ion optical array used here is designed to have an insulating support at the center to provide more structural support; in the analytical program, this spacing is considered one of the variables. Because it is relatively simple to modify this spacing in the hardware, the final choice of electrode separation need not be made at this time.

7. Material

Because its high thermal conductivity, low sputtering coefficient, good strength characteristics at high temperatures, and fairly good machinability, molybdenum was chosen as the electrode material.

C. Results from the Analog Computer Studies

The analog computer has been used in conjunction with the wedge shaped electrolytic tank to determine the ion trajectories, the position and form of the "upstream" plasma boundary, as a function of electrode displacement. The analog computer was used for initial studies so that time might be saved on the digital computer by starting from a partially converged solution.

The shape of the boundary for the unperturbed geometry was found to be almost spherical, with a radius of approximately 2.7 d, where d is the screen-accel spacing. A further case with a 20% displacement of the accel electrode toward the screen was also determined. It was found that this movement caused the shape of plasma boundary to deform to some extent and shift its position on axis by approximately 0.1 d in the same direction. The downstream plasma boundary has not yet been determined, and thus the change in total thrust cannot be calculated. The information concerning the emitting plasma is now being used to determine the downstream boundary.

D. Digital Computer Program and Result

A digital computer program which solves the trajectories of electrons from guns with rotational symmetry has been obtained. This program was originally written for NASA by C. Bogart in Fortran II language. The program has since been translated into Fortran IV suitable for use on the GE-635. The basic program uses finite difference techniques to solve Laplace's and Poisson's equations using boundary data specified by the user. In order to specify these boundary data, the area of the accelerator is overlaid with a suitable mesh and the potential at each mesh point (up to 3600) is calculated in terms of its neighbors. Hence the Laplace equation

$$\nabla^2 V = 0$$

at point R, Z within the problem becomes

$$RV_{R-1,\,Z} + RV_{R,\,Z-1} + (R+1/2)\,V_{R+1,\,Z} + (R-1/2)\,V_{R,\,Z+1} - 4RV_{R,\,Z} = 0$$

in terms of finite differences, where V_{ij} is the potential at the mesh point R, Z. The ion source is then divided into segments of equal length and the emission is determined by Child's law, using the potential as calculated above at a fixed distance (usually three mesh units) from the surface. The trajectory of a characteristic ion from each segment is then determined using the electric fields associated with the Laplace solution. Charges appropriate to the current flow can then be set in at each mesh point. The full Poisson solution can then be determined in terms of finite differences. The above process is then repeated until the solutions converge.

In order to be able to use the existing program for this study, it has been necessary to modify it in a number of ways. It was necessary to rewrite those sections dealing with rotational flow exclusively so that cases of planar symmetry could also be solved. This has involved rewriting the finite difference and the current continuity equations. In addition, because the emitting surface in this case is a plasma, sections had to be included which would allow the trajectories to be started from a generalized nonspherical surface. In order to do this a routine was written which first determines the length of the emitting surface from the input parameters, then divides the surfaces into a given number of segments, and finally calculates the normal direction at the midpoint of each segment. Using this routine the trajectories can be started at specified distances normal to the surface. An additional facility has been included so that the trajectories can be started from user specified positions. The writing of the program took somewhat longer than had been anticipated because several rather subtle errors were found in the program made available to us. This program has passed through several hands since its inception.

The location and shape of both the upstream and downstream plasma boundaries must be determined before the complete geometries can be run. The upstream boundary was determined in the analog computer, using the requirement of zero current density variation across the emitter as the boundary condition. The boundary thus found has been run on the digital computer; Fig. 2 shows the extent to which uniform current density has been achieved. Trajectories calculated by the computer are shown in Fig. 3, with an assumed downstream boundary.

Work is currently in progress to determine this downstream boundary. An initial estimate of its location is obtained using the planar diode formula[3]

$$\frac{s}{d} = (1 - R^{-1/2})^{1/2} \quad (1 + 2R^{-1/2})$$

where

$$R = \frac{|V_2 - V_1|}{|V_2|}$$

The dimensions and voltages are given in Fig. 4; the final shape and position of the surface will be determined from the equipotentials in this region. It has been found that the shape of the trajectories at distances less than d from the emitting surface is unaffected by moderate changes in the terminating conditions. This enables the downstream boundary to be solved independently of the upstream portion of the beam.

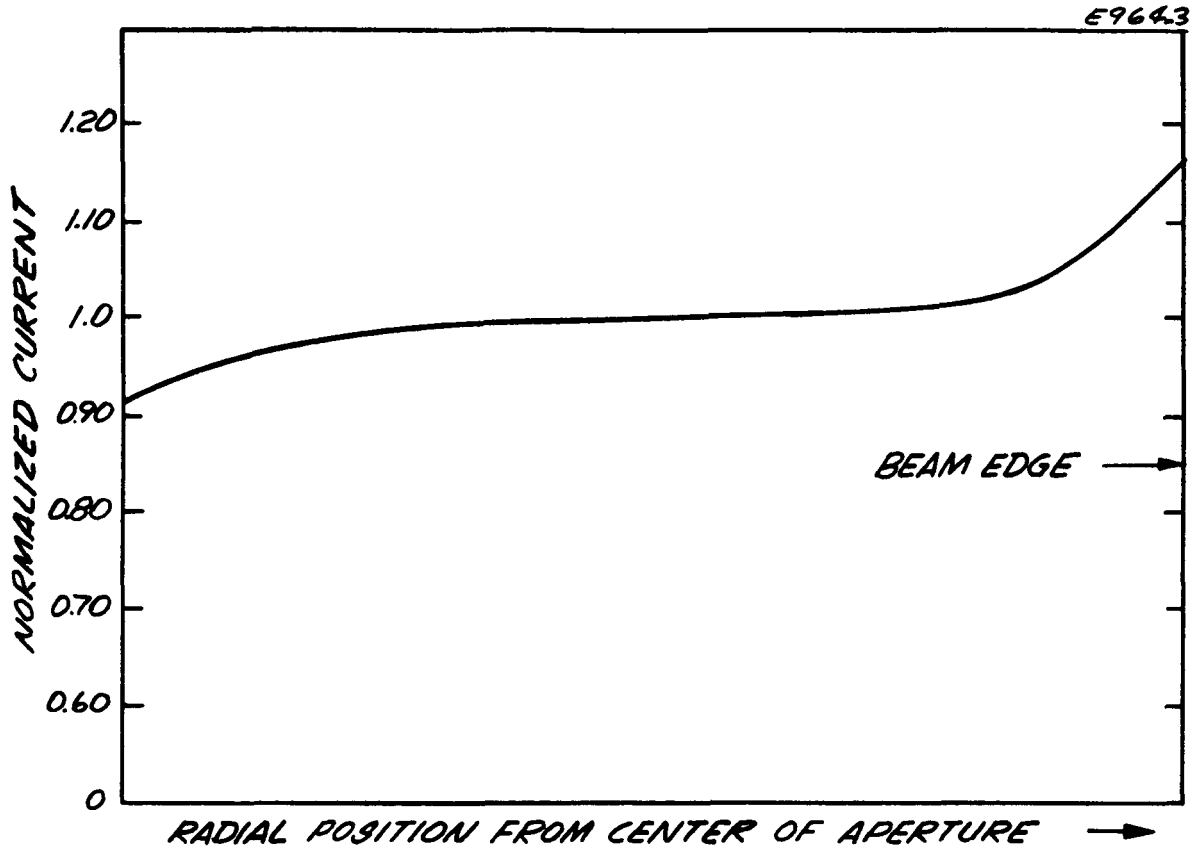

Fig. 2. Current variation at the emitter.

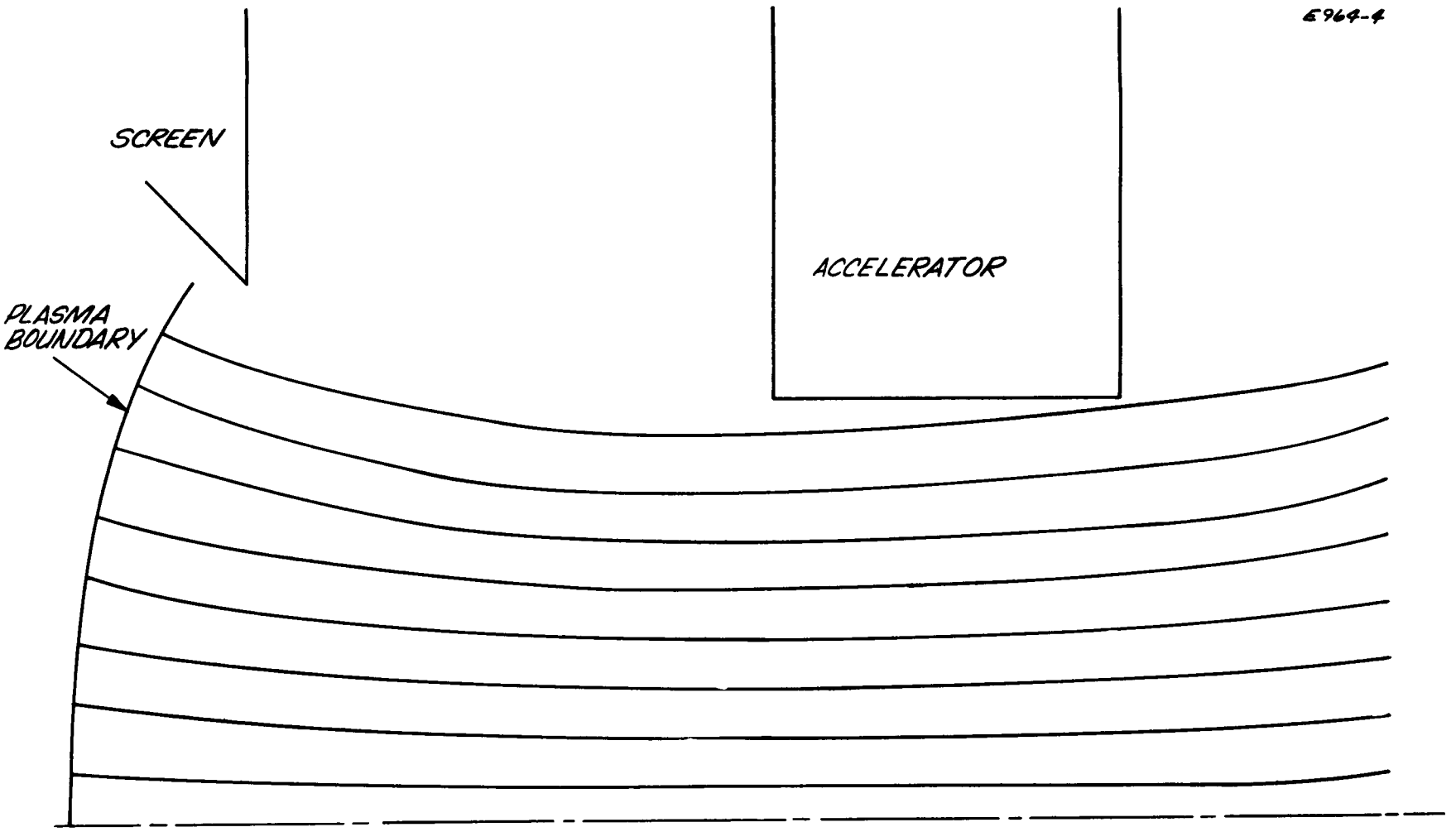

Fig. 3. Trajectories from unperturbed gun.

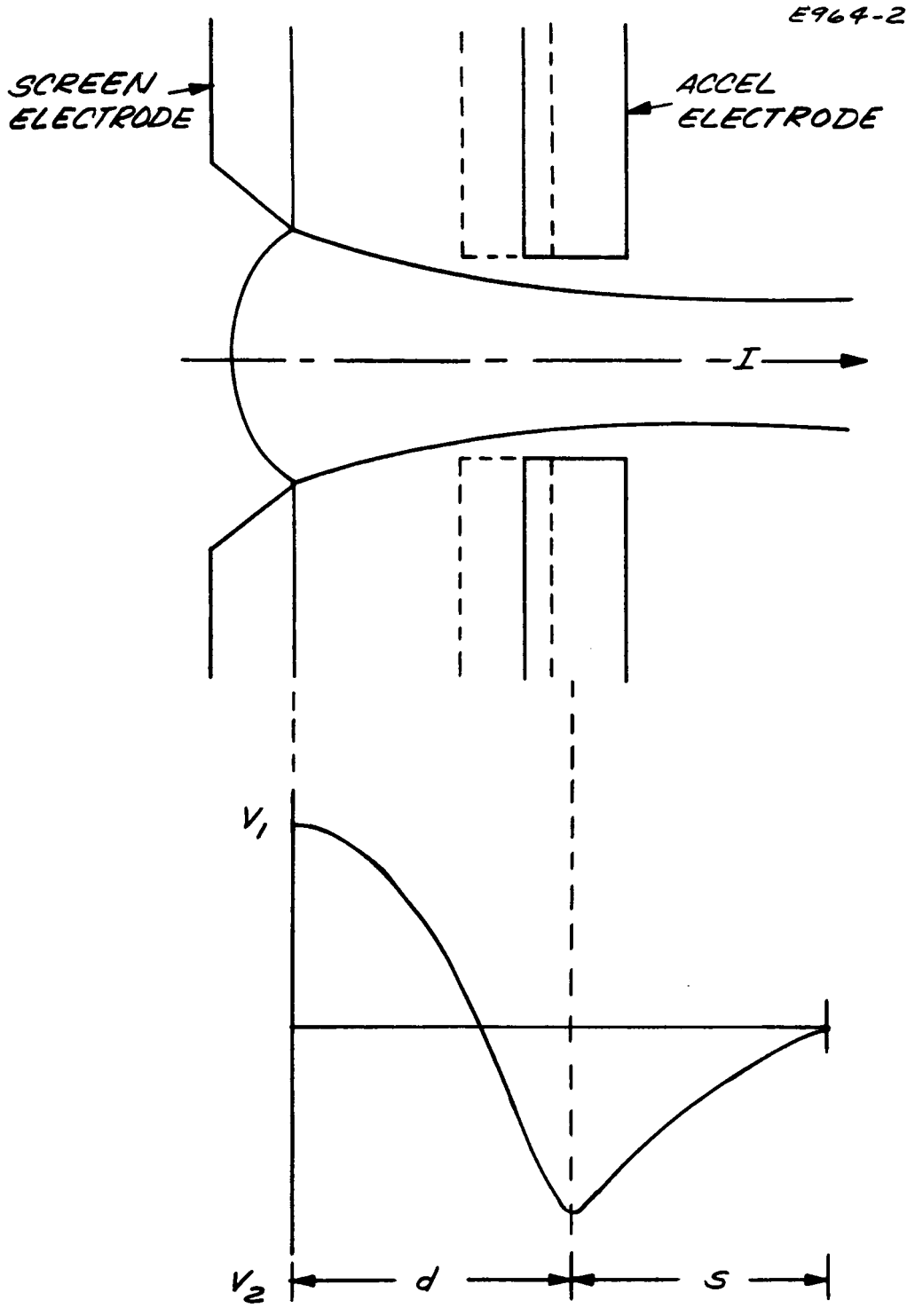

Fig. 4. Ion gun showing accel perturbation and idealized potential profile of planar gun.

III. CAUSES AND MAGNITUDE OF ELECTRODE MISALIGNMENT

This task is concerned with an analysis of the several factors in thruster assembly and operation which can cause distortion and misalignment of the electrodes, and a first order analysis of the effect of these misalignments in beam direction. Subsequently, the degree of electrode misalignment expected from this task will be coupled with the data on beam direction and magnitude obtained from the ion optical task to provide a complete analytic estimate of the thrust vector misalignment.

In this task two guidelines become apparent and will be followed whenever possible:

1. The analysis should be general enough to include all of the significant causes of misalignment
2. The analytical models should provide solutions which are sufficiently accurate to guide and correlate with the future experiments.

The accuracies of measurements and calculations which are required to be consistent with assumptions made in the analysis can be checked as the analyses proceed. A simple example of such a check on the magnitudes of grid displacements and rotations which are consistent with small thrust vector deflections will be given when the first ion optical model is available.

The electrode misalignments caused by thermal stresses appear to be the most difficult to analyze. We wish to develop analytical models which predict the misalignments which result from the asymmetric heat loading of initially aligned grids and the symmetric heating of initially misaligned grids. We begin by studying the thermal-stress problem in a conventional (aligned) electric bombardment engine.

A. Grid Displacements Caused by Thermal Stresses

When a solid body is subjected to a heat load, thermal stresses develop which tend to deform the body into a new shape. If the deformations are large they will seriously affect the equilibrium temperature of the body and a coupled thermal-stress problem must be solved. However, if the deformations produced by the thermal stresses are small, the thermal analysis and stress analysis become uncoupled and the problem is simplified. In this case the temperature distribution produced by the heat load is found for the undeformed body. The stresses and deformations are then calculated using this temperature distribution. The validity of the assumption of "small deformations" is easily checked by showing that the deformations do not cause any appreciable change in the temperature distribution of the body. In an operating electric bombardment ion engine the largest deformations which occur are the warping (bowing) of the electrodes. It will be assumed (and later verified) that the deformation of the electrodes is small (in the sense described above), so that an uncoupled thermal stress analysis can be performed.

B. Thermal Analysis of an Electron Bombardment Ion Engine

Because no detailed analytical thermal analysis has ever been carried out for the internal heat balance in an electric bombardment ion engine and in addition because no detailed experimental data on the temperature distributions on the component parts of such an engine have ever been taken, a somewhat slow but careful approach to the development of an analytical thermal model has been undertaken. The heat transfer inside the engine is primarily by radiation; the main sources of heat are the arc discharge and the cathode heater. An analytical effort is now under way to determine the appropriate view factors which come into the calculations of the radiative heat balance. An example calculation is now given.

Anode to screen view factor

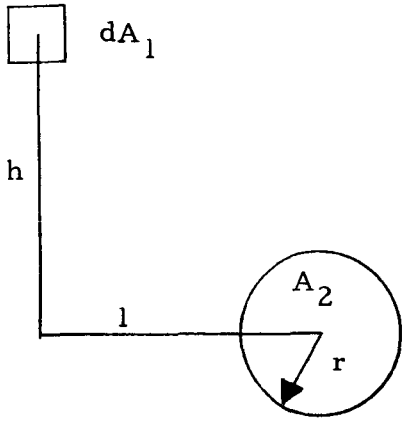

The view factor between the area element dA_1 and the circular disc of radius r is given by Eckert[4] as

$$F_{12} = \frac{h}{2}\left\{\frac{h^2 + r^2 + 1}{\sqrt{(h^2 + r^2 + 1)^2 - 4r^2}} - 1\right\} .$$

By integrating F_{12} over a cylinder of unit radius and height h we obtain the view factor

$$\overline{F}_{12}(h, r) = \frac{1}{4h}\left\{\sqrt{(h^2 + r^2 + 1)^2 - 4r^2} - (1 - r^2)^2 - h^2\right\}$$

from a cylinder to a concentric disk of radius r. This result can be checked against a previously known view factor $f(h, R)$ which governs radiation from the end of a cylinder of radius R and height h to its walls:

$$f(h, R) = \left(\beta + \frac{\beta^2}{4}\right)^{1/2} - \frac{\beta}{2} , \quad \beta = \left(\frac{h}{R}\right)^2 .$$

The reciprocity condition to be satisfied is that

$$A_1 F_{12} = A_2 f \quad . \tag{1}$$

It is easily shown that (1) is satisfied when $r = l = R$. Because the temperatures are not constant on the anode and screen, these surfaces must be subdivided. For an axisymmetric temperature distribution the view factors from a cylindrical zone on the anode to an annular ring on the screen become relevant. Fortunately, these view factors are easily derived from the formula F_{12}.

C. Thermal Mockup Study

As stated above, the objective of the thermal analysis is to establish an accurate temperature pattern for the thruster under various operating conditions. From this thermal picture the mechanical stresses and finally the strains will be calculated. In principle, it is possible to predict the location of all the heat sources for various operating conditions and then with only a knowledge of the geometry and surface emissivities to calculate the resultant temperature distributions. It was decided, however, to check these results with a simple thermal mockup which could be readily instrumented to assure that the detailed stress calculations would be based on thermal profiles which matched the true operating conditions as accurately as possible.

The mockup used consisted of a sheet stainless steel structure fitted with an existing set of 24 cm diameter ion optics, which were the largest size readily available. Coaxial resistance heaters were installed to simulate the cathode and to heat the anode. Two anode heaters were used; one was distributed over the whole length uniformly and the other was concentrated at the screen end where the majority of the discharge power is assumed to impinge. Twenty-four thermocouples were installed to monitor the local temperatures on the thruster shell, on the anode, and across the screen and accelerator electrode diameters.

To date, data from ten different operating conditions have been tabulated and are currently being correlated with the analytical model.

IV. THRUSTER DESIGN

The purpose of this task is to design a thruster, to be used later for experimental verification of the analytical results described above. The results of this program are to be used in the design of solar electric powered ion propulsion systems for unmanned missions. Recent studies have indicated that the most probable thruster module size for such a mission is in the 2 to 3 kW range and that the effective specific impulse will be 3500 sec or lower, depending on the exact efficiency curve for the thruster chosen. Based on current performance data, a 30 cm diameter thruster will meet the lower limits set above, while further improvements in thruster performance (particularly in the perveance of the ion optical system) will make such a thruster cover more of the above range. To assure that the design of the thruster used in the experimental verification tests in Phase II is realistic, the thruster used will be based on the above performance objectives and furthermore will approximate the weight permissible for a flight design; it will be fabricated using techniques similar to those used in the construction of flight hardware.

Based on the above, it was decided in conference with the JPL Program Manager to perform the experiments using a 30 cm thruster of the design described in Section II-B, whose design weight should be approximately 11 lb. Construction should use sheet metal techniques whenever possible. The design chosen employs a thermionic oxide cathode as the primary electron source* because current JPL mission studies and in-house experiments primarily use this device. The experimental thruster design is essentially a scaled version of the SERT II thruster as described in a number of recent reports from

*Substitution of a thermionic hollow cathode should not greatly alter the design.

NASA-LeRC and is essentially complete.[5] Provision is made in the integration phase of the program to investigate briefly the more critical parameters (i.e., shape of cathode pole tip and magnetic collar) which are expected to affect the performance.

In order to minimize the weight, the use of aluminum compared with stainless steel was considered for the discharge chamber shell, anode, and other structural members. Stainless steel was chosen because (a) it is known to resist attack by mercury; (b) it is readily welded to the soft iron end plates, while aluminum must be rivetted; (c) no weight penalty is associated with the use of stainless steel because it may be used in very thin sections. The design of the ion optical system and reasons for choosing molybdenum were presented in Section II-B.

The estimated weights of the various components are listed in Table I.

Based on the perveance of the SERT II ion optical system or HRL data for the counter-sunk screen (which are very nearly identical), the power handling capability of the proposed 30 cm design is shown in Fig. 5 as a function of specific impulse.*

The program plan calls for a detailed thruster design of the type described above. Thermal and mechanical calculations to establish perturbations in the thrust direction will be based on this design. The actual thruster to be constructed in the Phase II program will be closely based on this design as well, but will be modified where necessary to permit the instrumentation to perform the measurements to be incorporated into the design.

---

*Assumes η_{mass} = 90%; accel/decel ratio is 2.5; and power conditioning efficiency = 90%.

TABLE I

Component Weight

Part	Material	Weight, lb		
		0.010 in.	0.020 in.	Components Independent of Sheet Metal Thickness
Screen Collar	CR Steel			1.13
Lower Ring	CR Steel			0.47
Outer Shell	Stainless Steel	0.94	1.87	
Anode	Stainless Steel	0.98	1.95	
Screen Pole Piece	CR Steel			0.42
Screen Electrode	TEM Molybdenum			0.71
Accel Electrode	TEM Molybdenum			1.96
Back Plate	CR Steel	0.51	1.02	
Cathode Pole Piece	CR Steel	0.08	0.15	
Magnets	Alnico V			2.56
Insulator Assemblies				0.49
Subtotal		2.51	4.99	7.74
Total		10.25	12.73	

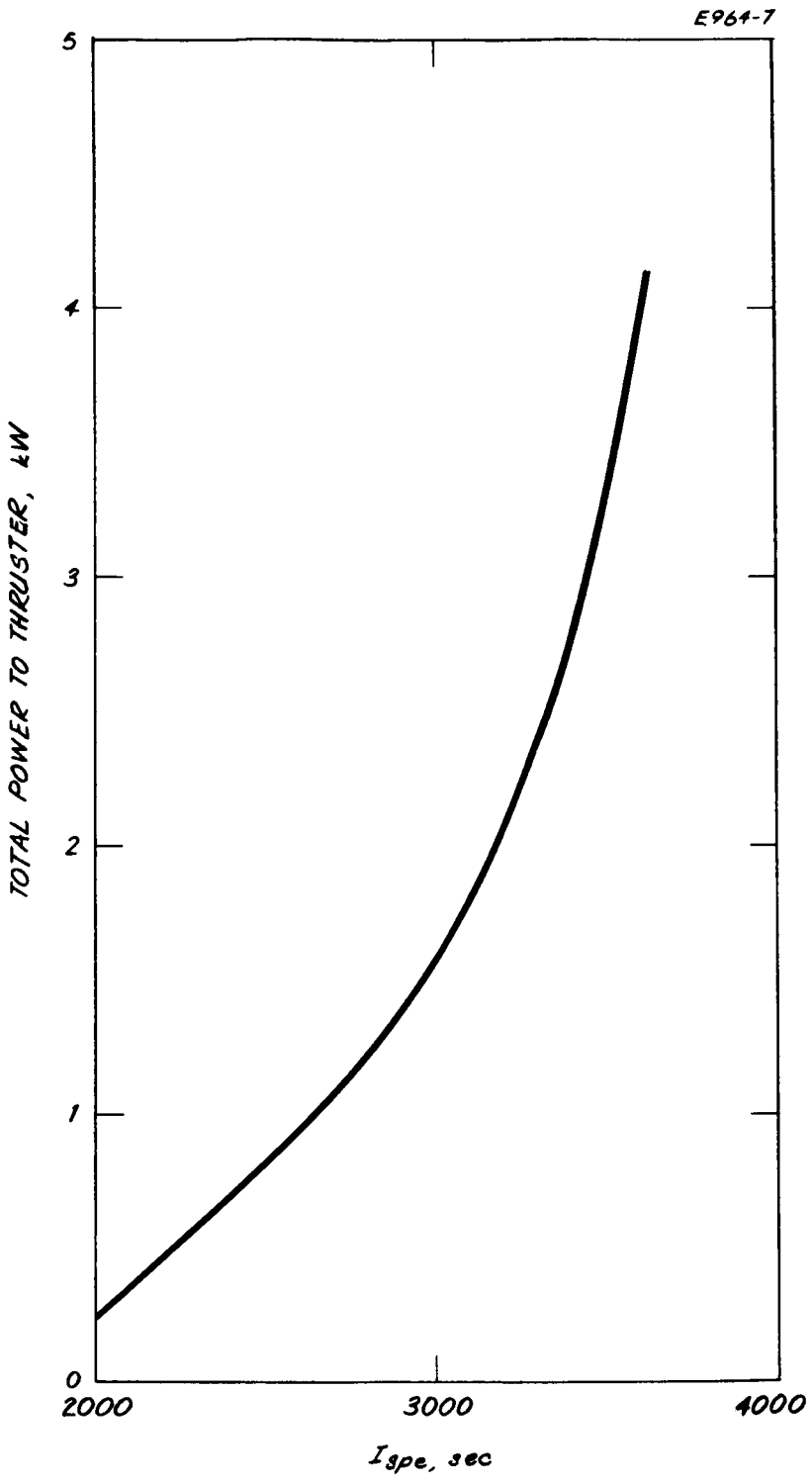

Fig. 5. Power handling capability as a function of specific impulse.

V. INSTRUMENTATION

A. Thrust Stand

In order to carry out the experimental verification phase of this program, a device is required to measure the location of the thrust vector from the thruster described above to within $\pm 1/4^{o}$ of angle and to determine whether any couple exists about the thrust axis to an accuracy of 5×10^{-4} in.-lb. Competitive techniques of making this measurement were analyzed. Conventional techniques for measuring either thrust or ion trajectories were investigated first. Each of these (viz., scanning Faraday cups, torsion wire suspension, and ion beam collection reaction) were eliminated for this application. At this point two new concepts of thrust measuring system were considered. It appears that each has sufficient sensitivity to measure the thrust vector directly, but that one may possess some inherent advantages. These two systems are discussed in detail below.

1. Survey of Possible Thrust Measurement Techniques

a. Stiff Column Design — The heart of this design is an extremely sensitive tiltmeter recently developed at HRL which is capable of resolving deviations of 10^{-9} rad from the horizontal. The basic concept is illustrated in Fig. 6. The thruster is so positioned that both the gravitational vector and the nominal thrust vector are parallel and lie along the axis of a slender hollow column which both supports the test package and contains the necessary electrical leads to operate the thruster. The base of the column is supported on a massive platform stabilized by a servo loop which is controlled by a tiltmeter. A second tiltmeter mounted on the platform supporting the thruster monitors small angular fluctuations which occur when variations in thrust direction cause the slender column to deflect.

The sensitivity of this system may be estimated as follows. The angular deflection of a slender column is given by

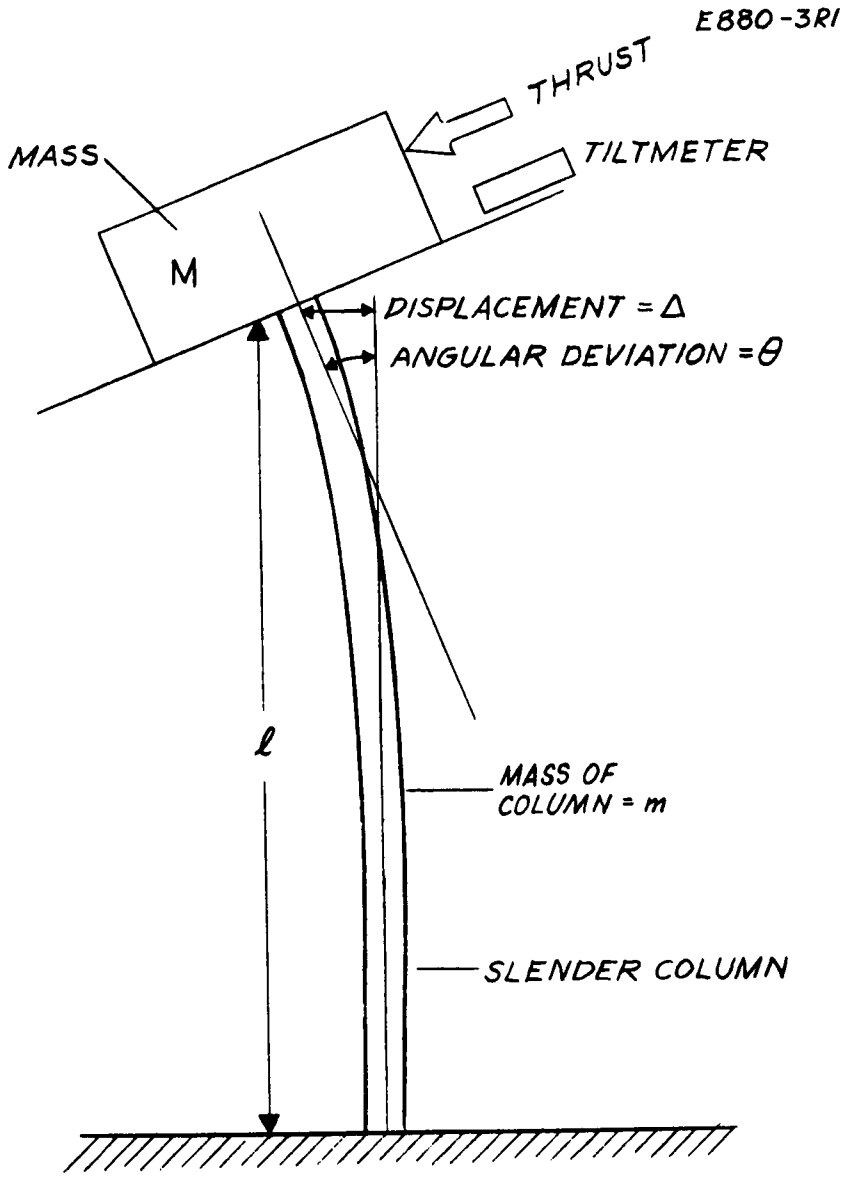

Fig. 6. Basic thrust measuring concept.

$$\theta = \frac{1}{2} \frac{F\ell^2}{EI} \quad \text{rad}$$

where

$F \equiv$ force perpendicular to column

$\ell \equiv$ length of column

$E \equiv$ modules of elasticity

$I \equiv$ moment of inertia of cross section of column

For a 6 in. long quartz rod, 1/4 in. in diameter, used in the proposal, $\theta = 10^{-2} F$. With the sensitivity of 10^{-8} rad specified for the tiltmeter, forces of 10^{-6} lb may be detected.

The basic concept of monitoring the position of a flat "pancake" shaped bubble formed in a liquid under a flat plate, which is the heart of the tiltment design, may be employed in two ways to achieve the desired result here. The first (Fig. 7) is to provide a servo system to maintain the platform on which the thruster is mounted in a level position using the bubble as an accurate null indicator. If the servo loop has been precalibrated it may be used to directly read out the force necessary to counteract that resulting from thrust deviations. The second (Fig. 8) technique is to use a complete tiltmeter which includes not only the bubble sensor but the necessary suspension and servo system to maintain the bubble in a level position on a moving platform and to indicate table declination directly.

This basic concept has sufficient sensitivity to measure thrust direction with the desired accuracy. A detailed analysis is necessary to choose the best physical design and to establish the sensitivity and stability of the system. Different mechanical configurations are required to measure angular deviations of the thrust vector from its desired position and couples about the thrust axis.

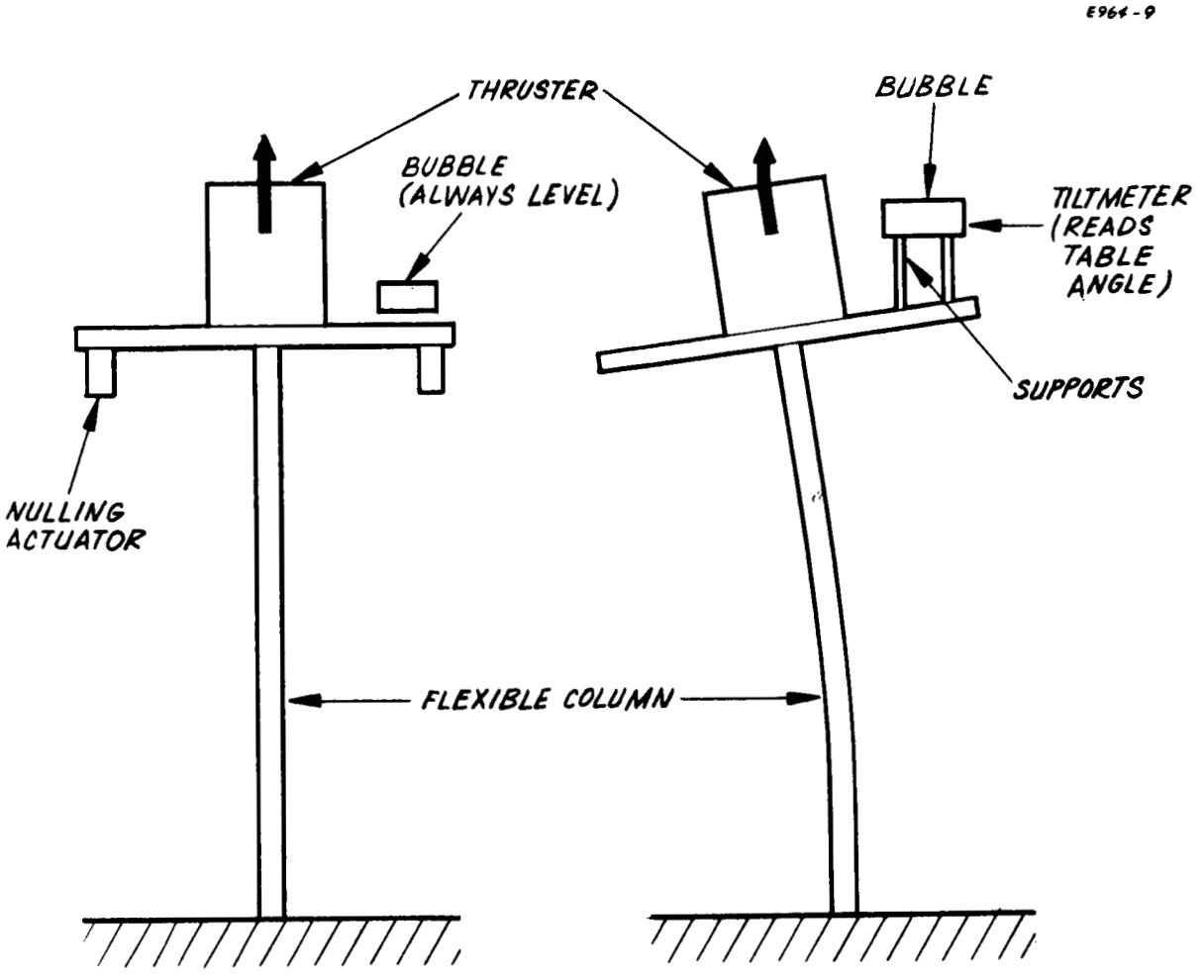

Fig. 7. Null producing system.

Fig. 8. Measurement of angular deflection.

b. Floating Suspension — This concept is an outgrowth of the thrust stand described above. By a different suspension mechanism it permits the three components of the thrust and the torques about the three mutually perpendicular axes to be measured* at the same time. The thruster platform is floated in a mercury pool and is free to drift horizontally or to lean away from the vertical, depending on forces applied. It is also possible for the system to rotate about its vertical axis if a couple exists about this axis. As discussed below, the suspension must be carefully designed to assure stability and to assure that the suspension itself introduces minimum perturbations into the system.

The operation of the system may be understood by referring to Fig. 9, which shows a two dimensional sketch of the essential elements of the device, and Fig. 10, which illustrates the two types of thrust misalignment which may occur. The mercury surface remains horizontal, thus removing the necessity of placing the whole apparatus on a stable table as in the previous design. In operation the table is releveled by the force motors F_z, using the tiltmeter as a reference, while horizontal and rotational motion is arrested by the force motors F_x and F_r, respectively. The position monitors which establish these null positions are not shown.

Consider first case 1 of Fig. 10. Here the thrust vector is at an angle ϕ with the desired direction along the centerline. It is apparent that such a force tends both to tilt the platform and to move it horizontally. To resolve such a force, force motors F_z level the platform and the force motor F_x compensates for the horizontal drift. Next, consider case 2 of the same figure which illustrates a situation in which the thrust vector has moved laterally while remaining parallel to the centerline. Notice that if $\ell_1 = \ell_2$, the same torque is produced about the center of rotation, as in case 1. However, there is no lateral

*The total thrust is calculated from electrical measurements.

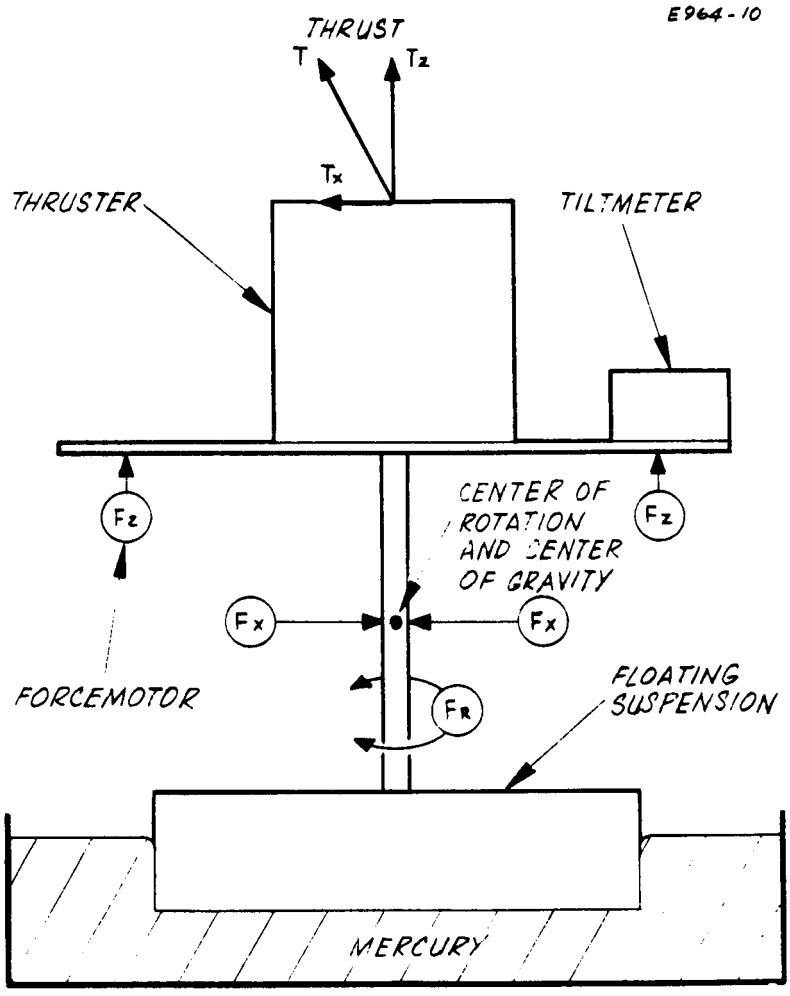

Fig. 9. Sketch of floating suspension device.

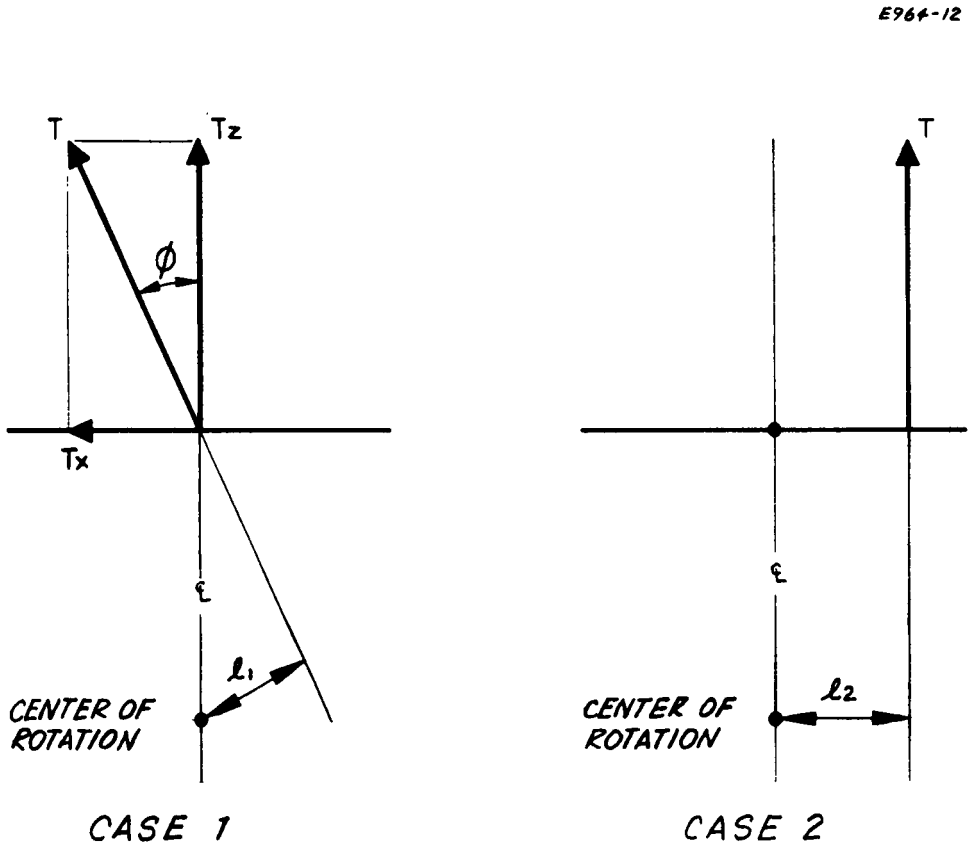

Fig. 10. Two types of thrust misalignment.

force in the second case. The ability to resolve these two cases is a distinct advantage over the stiff column design which can measure only the torque component and thus not distinguish between the two types of perturbation.

Measurement of the torque about the centerline tending to rotate the system is easily accomplished by the force motor F_r and a null sensor.

Thus, this system measures enough parameters to simultaneously determine all three orthogonal force components and all three orthogonal torques. A brief analysis of a practical design is outlined in Section V-A-2-b. However, because this system is a recent outgrowth of the stiff column design, its analysis is not yet complete.

In summary, this proposed system is superior to all others considered because it may simultaneously measure all six thrust and torque parameters that completely define the system.

c. Scanning Faraday Cup – The basic concept here is to use a Faraday cup to establish the number and direction of the ions at each point in the beam and from this information to infer the thrust direction. As with all the methods compared the limiting accuracy must be $\pm 1/4^{\circ}$. A fundamental problem associated with the various ways in which this general technique may be applied is that the ions in the beam do not follow laminar trajectories. For this reason, it is necessary actually to measure the direction that the ions are traveling at each point.

The most direct way to accomplish the above is to make the measurements at a point sufficiently far downstream that the actual source may be approximated by a point source. With the above required accuracy, the source must subtend an angle less than $1/2^{\circ}$ at the cup. For a 30 cm diameter thruster this gives a beam path length well over 100 ft. Not only are facilities of this size not available, but scattering in the beam would make the results uncertain.

The second possibility is to employ a Faraday cup relatively close to the thruster. The cup must now be designed to accept only ions which have emanated from an area on the source which subtends a $1/2^{o}$ angle or less at the collector. In other words, the cup must be preceded by a very narrow angle collimator. In principle at least, this device may now be used to measure experimentally the beam intensity as a function of angle (between Faraday cup beam axis) at each point in the beam. This measurement technique of course would generate an enormous amount of data. The experiment is difficult not only because of the accuracy required to position and control the location of the cup, but also because of the low signal level available ($\sim 10^{-8}$ A) after the selective collimation. Actually reconstructing the thrust vector from such measurements would no doubt require considerable computer analysis.

Another important factor which mitigates against this method is that collection of the data to establish a single thrust vector might require several hours, a period which is much longer than the stability of either the measuring equipment or the thruster.

In summary, it does not appear practical to construct the thrust vector to the desired accuracy from detailed measurements of ion trajectories in the beam. The principal difficulties arise from the very large amount of information required to define the beam with sufficient accuracy.

d. Torsion Wire Systems — The basic concept here is to hang the thruster from a thin wire and then measure the angle through which the wire twists because of the torque created by unbalanced forces. A number of variations of this general idea, such as suspending the thruster between two wires (as in a taut wire galvinometer) and using nulling techniques to maintain the net angular deflection at zero, all fall into this same general category.

With this type of suspension system it is conceptually possible to measure torques of the magnitude of interest here (5×10^{-4} in.-lb). However, there are a number of practical difficulties which seriously limit the application of the technique.

- Electrical Leads – A number of electrical connections must be made to the thruster. Each of these will stiffen the suspension and reduce sensitivity. A possible solution is to allow each lead to dip into a separate mercury pool, thus providing a friction free contact. It is very difficult to estimate the chance of success of this technique; it is at best a very cumbersome one.
- Stability – this arrangement is very susceptible to pendulum type instabilities. In principle, these can be damped out, but only with a sacrifice in over-all system response.
- Nulling Mechanism – Considering the device as a simple pendulum, it may be shown that the engine thrust (25 mlb) will cause motions of the thruster system of the same order of magnitude as those created by the torsional forces about the wire axis which we are trying to measure. This system thus requires a relatively sophisticated nulling system which automatically balances the main thrust vector at all times while at the same time measuring the much smaller (by a factor of approximately 100) force necessary to compensate for the thrust variation which we wish to measure.

- Interpretation of Data – A system such as this would be designed to measure only the torque about the axis of the suspension wire. Inherent in the system are a number of other degrees of freedom which may be excited by perturbations in the thrust direction. Coupling between these may make interpretation of the experimental results very difficult.

In summary, while this type of system conceptually has just sufficient sensitivity to measure the torque specified (5×10^{-4} in.-lb), a number of practical problems make application of the basic principle difficult, if not impossible.

e. Collectors – Under ideal circumstances it is possible to measure thrust produced by an ion thruster by measuring the effect that the impinging ions have on a collector. The principal practical difficulties which arise are associated with the dissipation of the beam power (~2 kW must be carried away from the collector by some type of forced cooling system, usually water). It is impractical to consider water leads with sufficient flexibility to permit the collector to respond to thrust levels of the magnitude of interest here. Therefore, it is not possible to measure the thrust direction by observing the reaction of the collector to the thrust.

2. Detailed Analysis of Two Most Promising Designs

a. Stiff Column Table Design – Even though the complete mechanical design is not yet specified, a number of parameters exist which are common to all concepts. The following example illustrates several of these points.

- resolution of thrust deviations of $\pm 1/4^{o}$

  for a 25 mlb thrust level, this is $\sim 10^{-4}$ lb of thrust transverse to the primary thrust vector.
- long term stability
- compatibility with the thruster operating environment
- direct readout (if possible).

Tiltmeter Sensitivity – The rated sensitivity of the standard 4 in. tiltmeter is 10^{-8} rad with higher sensitivity possible by using digital recording and time averaging. A very crude experiment with an "off the shelf" demonstration device indicated that a resolution of 5×10^{-8} rad was readily achievable with no special equipment. It will be shown in the following calculations that a sensitivity of 10^{-7} rad is adequate to measure a thrust component of 10^{-4} lb.

Design Equations – For the setup shown in Fig. 7

$$\theta = \frac{1}{2} \frac{T\ell^2}{EI} \text{ rad} \tag{2}$$

$$\Delta = \frac{1}{3} \frac{T\ell^3}{EI} \text{ in.} \tag{3}$$

$$P_c = \frac{\pi^2 EI}{4\ell^2} \tag{4}$$

$$f = \frac{1}{2\pi} \left[\frac{1}{(M + 0.23\ m)\ell^2} \right]^{1/2} \left[(2.38) \frac{r^4 E}{\ell} - Mg\ell \right]^{1/2} \tag{5}$$

where

$\theta \equiv$ angular deviation (rad)
$\Delta \equiv$ total deflection (in.)
$P_c \equiv$ critical buckling load (lb)
$f \equiv$ fundamental frequency (cps)
$T \equiv$ force $\perp$ to column (lb)

ℓ ≡ column length (in.)

E ≡ modulus of elasticity of column material (psi)

I ≡ moment of inertia of cross section of column = $1/4\ \pi\ r^4$ for round column ($in.^4$)

M ≡ mass supported on the column (slugs)

m ≡ mass of column (slugs)

r ≡ radius of column (in.)

g ≡ gravitational constant .

Design Example — Assume

$\theta = 10^{-7}$ rad for $T = 10^{-4}$ lb

$E = 3 \times 10^7$ psi (stainless steel)

$\ell = 12$ in.

Solving (2),

$$I = 2.4 \times 10^{-3}\ in^4 \quad . \tag{6}$$

For a mass of 1 slug (32.2 lb), the natural frequency, is, from (5),

$$f = 1.8 \text{ cps} \quad . \tag{7}$$

If we further assume that the supporting column is actually a tube with a wall thickness of 0.020 in., eq. (6) gives

r = 0.35 in., or a tube with

o.d. = 0.74 in.

i.d. = 0.70 in. (8)

The critical buckling load is a 12 in. long tube described by (6) is, from (4),

$$P_c = 1250 \text{ lb} \quad . \tag{9}$$

This first cut gives a design acceptable in all respects for the proposed task. There is, of course, a good deal of flexibility to choose other parameters should more detailed design place further constraints on the physical size or frequency response of the system.

There are two basic types of nulling actuators device which may be used to return the table to a level position as defined by the bubble: (1) a force motor, which is a device such as voice coil-magnet combination which generates a force which is independent of position; (2) a displacement motor, such as a magnetostrictive or thermally controlled element which changes in length in a controllable manner.

The distinction between these two types of device is important here because of the different manner in which they affect the suspension system. For example, in the system shown in Fig. 7, where both the bubble indicator and the table on which the thruster is mounted are supported on the flexible column and continuously leveled, it is important that a force motor be used because the inherent high compressive strength of the displacement type device will make the suspension system very stiff and seriously reduce the accuracy of the system. On the other hand, the leveling mechanism in the tiltmeter in a system of the type shown in Fig. 10 would likely employ a bubble system supported on three magnetostrictive rods which serve the dual purpose of supporting and leveling the bubble.

A voice coil consists basically of a current carrying coil suspended in the annular gap of a permanent magnet. The force equation is

$$F = B\ell I$$

where

$F \equiv$ force
$B \equiv$ magnetic field
$\ell \equiv$ length of wire in field
$I \equiv$ current flowing in wire .

For a typical 5000 G field, a current of 1 mA flowing through 3 ft of wire produces the desired 10^{-4} lb of restoring force.

The change in length for magnetostrictive materials is given by

$$\Delta \ell = \ell \lambda B$$

where

$\Delta \ell \equiv$ change in length

$\ell \equiv$ length of material in magnetic field

$\lambda \equiv$ magnetostrictive coefficient (usually a function of B)

$B \equiv$ magnetic field strength.

Values of λ vary widely for different materials ranging from 10^{-8}/G for cobalt over a range from 0 to 4 kG to approximately 40 times this value for nickel over a range from zero to 100 G. As an example of the application of this principle, consider the restoring mechanism which levels a 2 in. diameter bubble that is tilted 10^{-6} rad. One support leg must then compensate by a change in length of 2×10^{-6} in. Assuming that a 1 in. long pure cobalt leg is used, it must be immersed in a field of 200 G.

As indicated above, the choice between these two types of device depends primarily on the total system design and the functional role that the nulling mechanism must play.

The system as described in Section V-A-1-a basically measures the deflection of a slender column caused by the component of thrust perpendicular to the column. It is important that extraneous torques caused by lateral displacements of the center of gravity of the system or of the thrust vector not invalidate the accuracy of the measurements.

Figure 11 depicts these perturbing forces. Ideally, the forces due to the thrust vector and the center of gravity should act along the axis of the supporting column. Displacements of these two forces from the ideal position are represented by x and y, respectively, in Fig. 11. The column of length ℓ is supported on an accurately level table and makes an angle β with the horizontal. Assume first that $\beta = 90^{\circ}$ and that the two perturbing torques (taken about point A at the base of the column) are

$$L_1 = (T \cos \alpha)(x)$$

$$L_2 = Mg\, y$$

where

$M \equiv$ mass of the system (assume 25 lb)
$T \equiv$ total thrust (assume 0.025 lb)
$\alpha \equiv$ thrust deviation ($\geq 1/4^{\circ}$) .

The torque produced by the thrust component that we wish to measure is

$$L_3 = T(\sin \alpha)\, \ell$$

where ℓ = column length (assume 12 in.). To assure that $L_3 > L_1$ and $L_3 > L_2$, we must have

$$x < \frac{(T \sin \alpha)\ell}{(T \cos \alpha)}$$

$$\therefore \quad x < 0.050 \text{ in.}$$

and

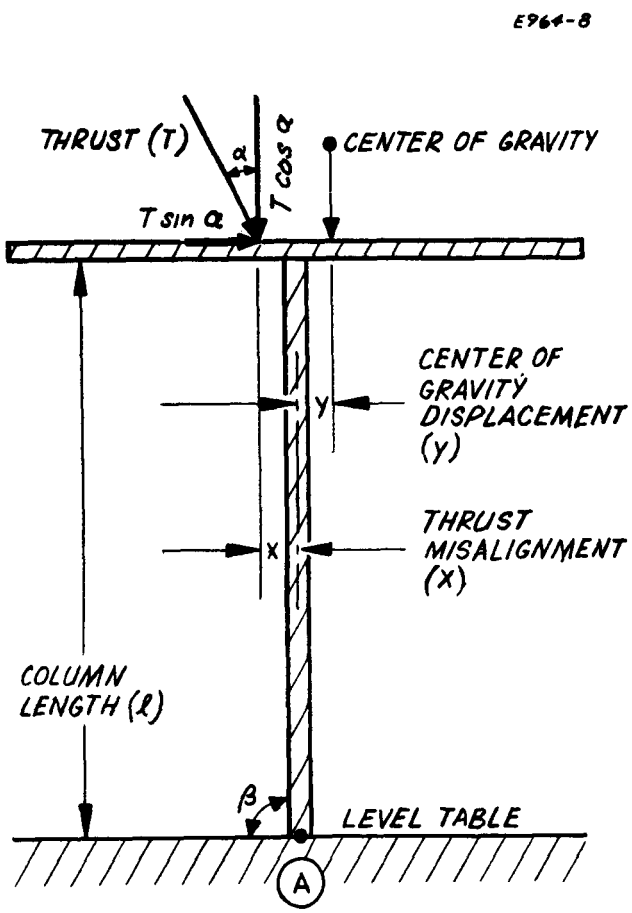

Fig. 11. Perturbing forces.

$$y < \frac{(T \sin \alpha)\ell}{Mg}$$

$$y < \frac{(25 \times 10^{-3})\,(4 \times 10^{-3})\,(12)}{25}$$

$$y < 5 \times 10^{-5} \text{ in.}$$

These calculations show that there is a relatively large tolerance on the alignment of the thrust vector with the axis of the supporting column, while very little shift in center of mass position is permissible.

Consider first the thrust vector misalignment. For a perfectly symmetrical thruster the thrust vector should pass through the exact center of the ion optical system. This can certainly be specified to better than the 0.050 in. permissible error calculated above. Determining the probability that a shift of this magnitude will occur during testing should be one of the goals of the analytical study. It is fortunate that reasonable tolerance to lateral shifts in the thrust vector location are tolerable, because it is not possible to separate the two torques L_1 and L_3 by varying the total thrust, since each varies directly with the thrust magnitude and angle. The only other variable which even in principle permits the separation of the two effects is the misalignment x. As shown below, this cannot be adjusted during a run because of the very large effects associated with shifting the position of the center of mass.

As shown above, the force on the thrust table due to gravity acting on the center of mass of the table and its load (the thruster, etc.) must pass accurately through the pivot point A at the base of the support column. Since neither the center of mass nor the pivot point can be located to the necessary accuracy, a technique for mechanically balancing the system is required. The location of the thrust vector physically defines where the thruster must be located with respect to point A; therefore, balancing must be done by the addition of weights to the table, possibly using one of the many techniques developed for modern analytical balances. Final precision balancing may be done with

automatic nulling incorporated into the system (of the type shown in Fig. 9) to maintain the bubble level during the test. This would show up as a zero offset at the no thrust condition.

Small shifts in the center of mass may occur during operation because material is being removed from or deposited on the ion source or its supporting structure. Other center of mass shifts may inevitably occur when the electrodes are moved with respect to each other as part of the experimental program. Assuming that the accelerator electrode is 1/20 the weight of the total system and that it is moved 0.010 in. during the experiment, this in effect shifts the center of mass 5×10^{-4} in., thus producing an effective torque an order of magnitude larger than the minimum to be measured. Fortunately this effect can be calculated and also measured directly by shifting the electrodes with no beam extraction and thus may be subtracted from the observed thrust deviation to give the true reading. Because the electrode mass and the amount of motion will be known, it is also possible to compensate for the center of mass motion by moving an equivalent weight in the opposite direction. The permissible tolerance for angle β may be directly calculated once the column length ℓ is fixed.

We now develop a mathematical analog of the stiff column system and calculate from it the system output and frequency response. The results of this analysis indicate that the example system designed above provides a 19 mV signal when the thrust vector is perturbed $1/4^{o}$. The frequency response is linear up to approximately 1 cps.

As stated above, the two axis level sensor is based on the kinetic properties of a gas bubble in a liquid confined under an optical flat. This sensor has demonstrated resolution on the order of 10^{-9} rad. The output of one axis of this sensor is given by

$$V_b = \lambda_b \frac{s^2 X + g \theta}{S(s + f_b/m_b)} \qquad (10)$$

where heavy bodied letters denote the Laplace transform of a time variable and

$S \equiv$ complex frequency variable

$V_b \equiv$ output signal, V

$\lambda_b \equiv$ gain constant

$\mathbf{X} \equiv$ one of the two horizontal coordinates of the bubble

$\theta \equiv$ angular tilt of the optical flat measured from the $\mathbf{X}$ axis

$g \equiv$ gravitation acceleration

$f_b \equiv$ viscous damping coefficient

$m_b \equiv$ effective mass of the bubble (considered as positive).

This sensor serves as the detector in a sensitive force measuring system shown in Fig. 12. Assuming small deflections, the differential equation for this system can be stated as

$$S^2 M + \mathbf{X} + S f_m \mathbf{X} + R_m \mathbf{X} + \mathbf{F}_m + \mathbf{F}_e = 0 \quad . \tag{11}$$

The system shown above consists of a test table mounted on a flexible cantilever strut. $\mathbf{F}_e$, the force to be measured, produces linear and angular motion of the table which is sensed by the bubble. The output of the bubble is fed back to the table by a force motor $\mathbf{F}_m$. Spring rates associated with the force motor and the cantilever strut are shown as km while all viscous losses are lumped under f_m.

The table tilt is related to the table deflection by the law of the uniform cantilever beam

$$\theta = \frac{3}{2\ell} \mathbf{X} \quad . \tag{12}$$

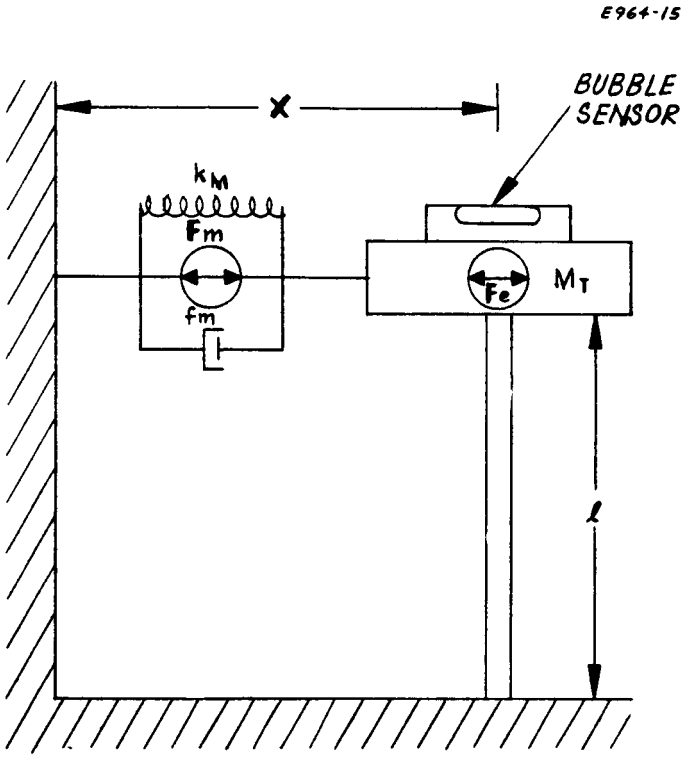

Fig. 12. Analog of thrust meter.

If the force motor output F_m is proportional to the bubble sensor output V_b, i.e.,

$$F_m = K_m V_b \quad ; \tag{13}$$

if a cascade lead compensating network is added such that the bubble sensor output (10) is now given by

$$V_b = K_b \frac{S^2 \mathbf{x} + g\theta}{S} \quad , \tag{14}$$

the transfer function relating V_b to the force F_e is

$$\frac{V_b}{F_e} \quad \frac{\frac{Kb}{Mt}\left(S^2 + \frac{3g}{2\ell}\right)}{S\left(S^2 + S\,\frac{fm}{Mt} + \frac{km}{Mt}\right) + \frac{Kb\ Km}{Mt}\left(S^2 + \frac{3g}{2\ell}\right)} \quad . \tag{15}$$

This transfer function is stable for all values of gain. A quantitative estimate of system performance may be obtained by selecting numerical values as follows.

In the weight of the table Mt the length and stiffness of the cantilever strut ℓ and km were dictated by mechanical design considerations (see above). The gain factors Km and Kb were selected to optimize the shape of the frequency response curve of the system. fm was selected based on a force motor with 10% of critical damping. $|F_e|$ is the magnitude of the minimum force to be resolved and $|V_b|$ is the magnitude of the system output signal under a steady state condition. With the numerical values listed below, the characteristic equation of the system can be factored to determine the location of the poles.

$K_m = 2.32 \times 10^{-2}$ N/V $\qquad \frac{3g}{2} = 48.2$ rad^2/sec^2

$\frac{km}{Mt} = 128$ rad^2/sec^2 $\qquad \frac{fm}{Mt} = 2.26$ rad/sec

$$\frac{Kb}{Mt} = 552 \text{ V/N sec}^2 \qquad Mt = 14.6 \text{ kg}$$

$$|F_e| \quad 4.45 \times 10^{-4} \text{ N}$$

$$\frac{Vb}{Fe} = 43 \frac{\frac{S^2}{48.2} + 1}{\left(\frac{S}{8.3} + 1\right)\left[\left(\frac{S}{8.6}\right)^2 + \frac{6.6}{8.6^2} S + 1\right]}$$

At $|F_e| = 4.45 \times 10^{-4}$, $|V_b| = 19.2$ mV for $S = 0$. The system frequency response, as shown in Fig. 13, is 3 dB down at approximately 0.5 Hz.

As described above, the system is sensitive to tilt and acceleration of the mounting base. Errors resulting from this sensitivity can be avoided by measuring the differential output of two identical systems, one carrying the equipment under test and the other carrying a dummy set of equipment. To the extent that the two systems have identical frequency response curves, motion of the mounting base causes no differential output (provided, of course, that this motion does not cause either system to saturate).

b. Floating Suspension — As stated above, this concept is a recent outgrowth of the stiff column design analyzed in the preceding section. Its primary advantages are (1) that it resolves the two possible types of thrust misalignment illustrated in Fig. 10 and (2) that a single experimental setup measures both angular deflections of the thrust vector and torques set up about the centerline or nominal thrust axis. Figure 14 illustrates the proposed suspension mechanism which provides the additional degrees of freedom.

It is desirable to design the floating suspension system so that the buoyant force of the mercury supports the platform but does not tend to force it to maintain a particular position. In other words, by proper mechanical design the system may be made critically stable so that the buoyant forces neither tend to right it or to upset it.

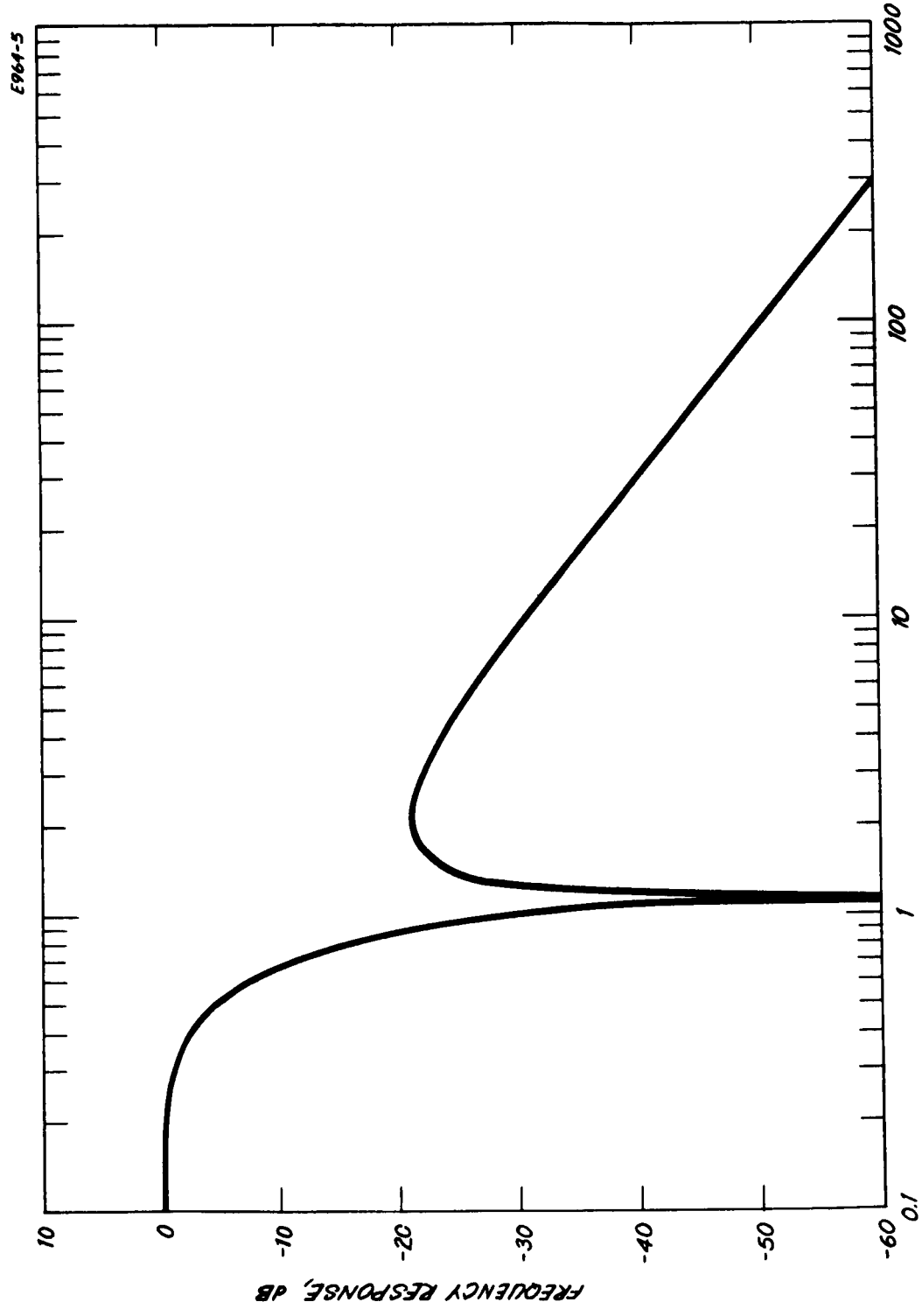

Fig. 13. Frequency response of proposed system.

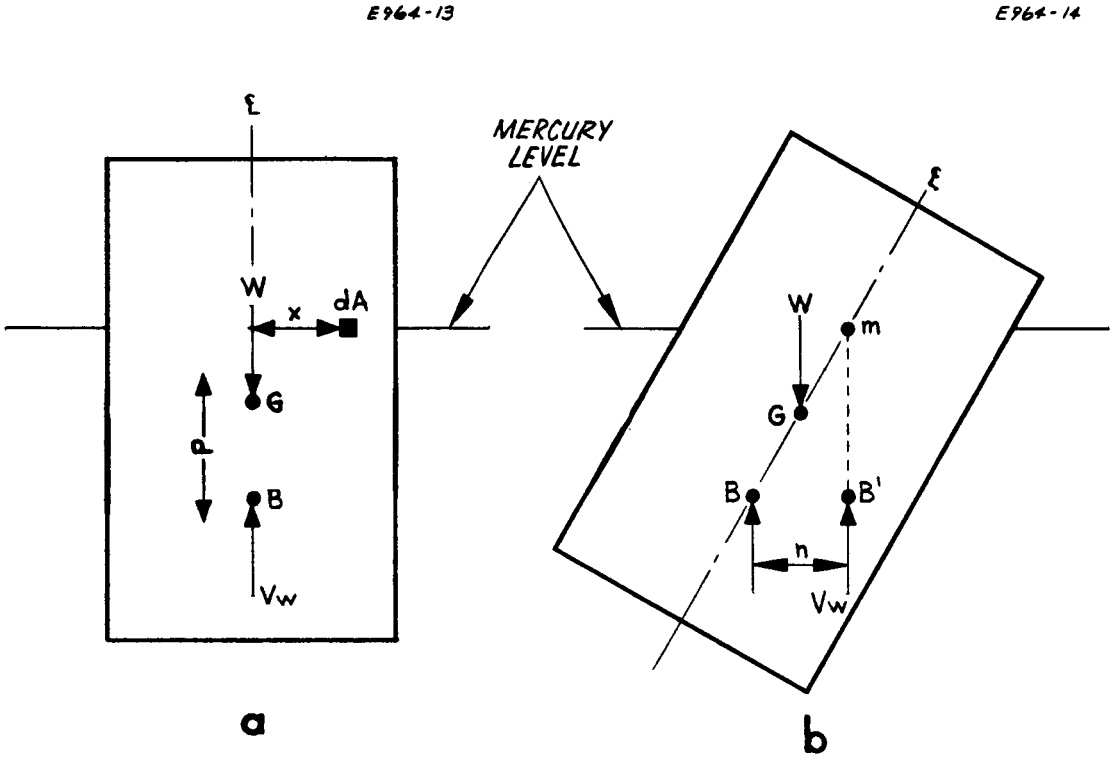

Fig. 14. Proposed suspension system.

Reference to Fig. 14 will make this more clear. In the upright floating body (Fig. 14 (a)) the weight w of the body acts through the center of gravity G and the buoyand force Vw* through B the center of displaced liquid. If the body is tipped as in Fig. 14(b), the volume of displaced liquid remains the same but the center of bouyancy moves to B' and the couple formed by W and Vw tends to right the body. The line of action of the bouyant force passes through the center line (BG) at m. As the angle of tilt approaches zero, m approaches a limiting position above G known as the metacenter. The distance Gm is known as the metacentric height. It is apparent from Fig. 14 that the greater as value of Gm increases, the couple which tends to right the body increases. Elementary tests on floating bodies show that for small angles of tilt the metacentric height is given by

$$Gm = \frac{I}{V} - P$$

where

P ≡ distance between the center of gravity and center of bouyancy

V ≡ volume of displace liquid

I ≡ area moment through a water line section of the floating body ($=2\int x^2 \, d\,A$ of Fig. 13(a)).

For our application we wish the metacentric height (hence the force tending to right a displaced floating body) to be zero. Therefore, from the above

$$\frac{I}{V} = P \quad .$$

All quantities may be calculated from a knowledge of the shape and specific gravities of the materials involved. Once this condition is achieved, the body is neutral.

*Vw ≡ product of displaced volume V and specific gravity of liquid w.

Electromagnetic force motors of the type described earlier are suitable for use here as well. They are positioned to compensate the thrust components as described in Section V-A-1. A small tiltmeter of the type described in the same section will be used to determine when the thrust platform is parallel to the mercury surface. The null meters necessary to determine when the side thrust component and torque have been exactly compensated have not yet been chosen. A high degree of sensitivity is not required because any continuous unbalanced force acting over a period of time will generate enough motion to exceed the deadband of even a relatively crude system. A complete mathematical analysis of this system similar to that described above for the stiff column system will be completed during the next quarter.

B. Electrode Position Monitors and Motion Generator

Two types of experiments are planned in the experimental verification phase of this program. The first is to precisely move the electrodes with respect to each other to generate the perturbations considered in Section II in a known manner. This requires mechanisms to precisely control the relative angular and lateral positions of the screen and accelerator electrodes. The second phase of the experiment is to run the thruster for a 50 hour period while monitoring both the direction of the thrust vector as well as the electrode misalignments that naturally occur as the run progresses. These tests require mechanisms to measure the relative positions and shapes of the electrodes. Final design of both the position monitor and motion generator awaits outputs from the study phase of this contract which will approximately define the range over which motion must be generated.

1. Position Monitor

Two types of position monitor are required. The first must measure the axial alignment of individual apertures in the screen and accelerator electrodes and the second and actual contour of the electrode surfaces. These measurements must be made in vacuum on a thruster while it is operating.

It was initially proposed that a light beam be used for each of these measurements. Differential detectors are available[6] which may be used to monitor the motion of a collimated beam of light to a few thousands of an inch. Further investigation indicated, however, that the task can be more simply done with a differential transformer of the type sold by Automatic Timing and Controls Inc., Type 6234. One such transformer was purchased, tested, and found to provide a response of

$$\frac{1.8 \text{ mV}}{(1.001 \text{ in.})\ (\text{primary volt})}$$

Further experiments indicate that cross coupling between motions in the orthogonal direction is attenuated by at least an order of magnitude.

Measurement of the electrode surface contours while the thruster is operating represents a relatively difficult task. It is proposed to accomplish this as shown in Fig. 15. A series of short pins will be set in the accelerator surface across a diameter. The relative positions of these pins will be observed from outside the vacuum chamber with an alignment telescope* capable of directly reading position to 0.001 in. over a ± 0.050 in. range. The screen position may be similarly monitored by mounting pins on the existing holes in the accelerator electrode. By blocking 10 to 15 of the nearly 3000 holes in the electrodes, a reasonably good measure of the electrode profile is possible. It will be necessary, of course, to block apertures symmetrically about the centerline so that thrust perturbations do not result.

*K&E type 712020 available at HRL.

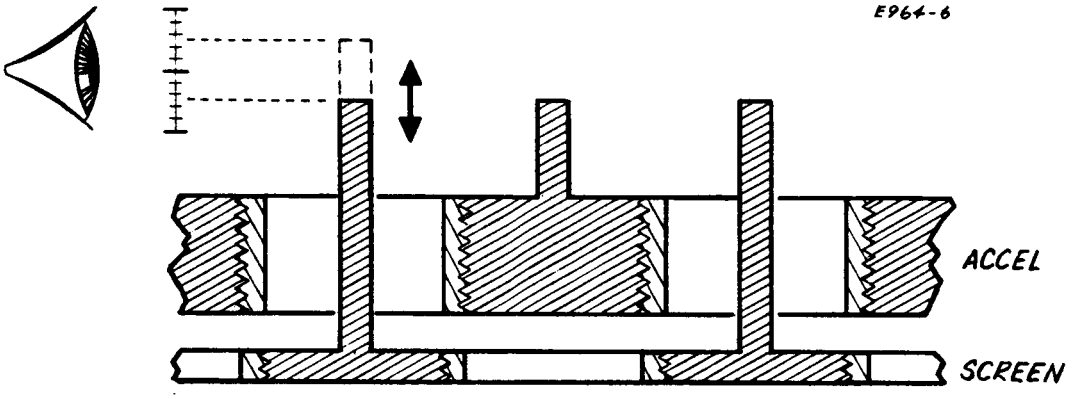

Fig. 15. System to measure electrode warping.

2. Electrode Motion Generator

Details of the motion generator have not yet been worked out. It is tentatively decided to employ a mechanism based on the differential expansion of dissimilar metals.

VI. CONCLUSIONS

All elements of the program are on schedule according to the original program plan. The digital computer program used in the ion trajectory determination required somewhat longer than anticipated for debugging, but it is now running satisfactorily. A new concept for a thrust measuring system has been conceived and is being evaluated. Although certain parts of the analysis of the slender rod thrust stand may be inapplicable, it is felt that the floating table system will prove more effective and economical for the experimental phase. No problems of significance, other than those mentioned above, have arisen. It is anticipated that the program will be completed on schedule.

VII. PROGRAM FOR NEXT QUARTER

The ion optical study will be completed during the next quarter. The analog computer technique will be phased out early in the quarter, after completing its objectives, and the main body of data desired from this effort will be generated by the digital computer.

The analysis of causes and magnitudes of electrode misalignments will be carried out, based partly on the results of the thermal simulated-thruster tests.

The design of the thruster system, to be used in the experimental verification tests and including the thruster and the electrode position adjustment and monitoring devices, will be essentially complete by the end of the next quarter.

VIII. NEW TECHNOLOGY

In the first three months of the contract period two novel techniques for thrust measurement have been studied and evaluated. To date no hardware has been constructed to actually demonstrate the technology.

REFERENCES

1. R. T. Bechtel, "Discharge Optimization of the Sert II Thrustor," AIAA Propulsion Conference, Colorado Springs, 1967, No. 67-668.

2. S. U. Pawlick and P. D. Reader, "Accelerator Grid Durability Tests of Mercury Electron Bombardment Ion Thrustors," NASA TND-4054, 1967.

3. C. Foy, A. L. Samuel, and W. Shockley, Bell System Tech. Rev. 17, 49 (1938).

4. E. R. T. Eckert, "Heat and Mass Transfer," 1959.

5. R. T. Bechtel, et. al., "Performance of a 15-cm Diameter Hollow Cathode Kaufman Thrustor," NASA TMX-52376, 1968.